Fluid mechanics of viscous flow down a slope

ISM Report

Divasjyoti Parashar
Tatsam Garg

Ashoka University
15th May, 2021

Introduction

When a broad band of viscous fluid is released from a cuboidal reservoir onto a plane sloping surface (as seen in figure 1), the nature of the flow is found to change with time. From a plane horizontal flow front initially, the flow breaks up into finger-like or wave-like instabilities, the amplitude of which are only seen to increase with time. In this experiment, we delve deeper into this nature of fluid flow where the formation of instabilities and their evolution with time is of much interest to us. In our study, we have limited ourselves to the case of 'constant volume flow'.

Our study is motivated by Herbert E. Huppert's work published in 1982 titled "Flow and instability of a viscous current down a slope". In our study, we essentially try to reproduce and verify the results obtained by Huppert and add our own analysis of the same. The flow we are studying is resemblant of natural phenomena such as the flow of lava down a volcanic mountain or glaciers down a slope and this resemblance is indicative of the importance of studying a phenomenon such as this.

Literature Review

This study uses the experimental schematics introduced by Herbert Huppert [Nature 300, 427(1982)]. Consider an inclined plane surface. A fixed volume of a viscous liquid is released on this surface from a cuboidal reservoir placed at its top. Initially, the liquid flows downward with a horizontally uniform front, provided horizontal symmetry is ensured experimentally. We call this the stable regime. After some time, the advancing front develops random instabilities, which gradually take the form of periodic finger-like projections as shown in figure 1. We refer to this as the unstable regime.

Huppert calculated that the advancing coordinate, x, of the uniform horizontal front in the stable regime follows the equation:

$$x = \left(9A^2 g \sin\alpha / 4\nu\right)^{1/3} t^{1/3} \tag{1}$$

where α is the angle of inclination, A is the lateral area of cross section (it is a measure of the total volume of liquid being released), g is the acceleration due to gravity, ν is the viscosity and t is the time.

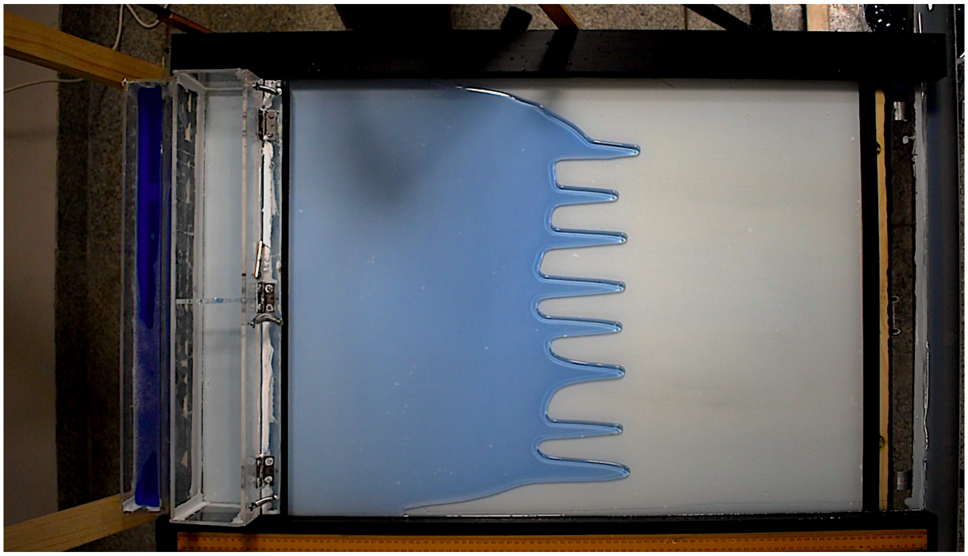

Figure 1: Experimental set-up for viscous fluid flow on an inclined plane.

For the unstable regime, Huppert calculated that the wavelength of the projections/protrusions/rivulets (Silvi *et al.*, 1984) is given by:

$$\lambda = 7.5 \left(A^{1/2} T / \rho g \sin \alpha \right)^{1/3} \tag{2}$$

where T is the surface tension of the liquid and ρ is the density.

The experiments led to the following conclusions (Silvi *et al.*, 1984):

1. In the stable regime, the dynamics is governed by the balance between the viscous and gravity forces.
2. In the unstable regime, surface tension dominates over viscosity in determining the wavelength of the projections.
3. The length scale which the fluid front flows stably before the instabilities kick in is proportional to $A^{1/2}$, and thus, related to the total volume of the liquid. This is inherently tied to the fact that surface tension effects dominate as the fluid layer becomes thinner. Larger volume of fluid translates to a longer distance covered by the fluid front before the fluid layer becomes thin enough for surface tension to dominate.

In our study, we verify the above results using a similar experimental set-up. Further, we explore two different analytical techniques to characterize the process of development of instabilities— Analysis of the fastest growing mode in the fluid front and a phase transition picture for the transition from stable flow to instabilities.

Experiment

The study required us to observe the flow of a broad band of viscous fluids down a plane sloping surface. The experiment was performed for three fluids of different viscosities and for three different angles of inclination of the ramp. The details of the experimental setup and the experimental process have been mentioned below. We have added a section that talks about the challenges faced during the experimentation and how we dealt with them. Please refer to Appendix B for detailed design of the apparatus.

Experimental Setup

The experimental setup consisted of an inclined glass ramp with a cuboidal reservoir at its head, spanning the width of the ramp. The ramp and the reservoir were held in place by a wooden framework. An openable gate, when hooked, kept the content of the reservoir from flowing onto the ramp. Three springs attached to the gate ensured that the entire gate would open immediately without delay when unhooked. The angle of inclination of the ramp could be changed at will by means of a rotating lever that was attached to two sliders that supported the ramp (refer to images in Appendix B). We also placed a boundary structure on each side of the ramp to prevent the fluid from flowing over the sides. A camera stand was placed such that we could get a top-down view of the ramp. The angle of the camera could be adjusted according to the angle of inclination of the ramp.

Conducting the Experiment

We prepared three fluids of varying viscosities in the lab. We used water, medical-grade glycerine and food-grade liquid glucose for the preparation of the fluids. Liquid glucose is an aqueous solution of nutritive saccharide obtained by starch hydrolysis, often using corn and rice as raw material. Water could be added to liquid glucose in varying amounts to change the viscosity of the resultant fluid mixture.

1. Glycerine - medical grade glycerine [$\nu = 9.5$ Poise]
2. Glu_150 - 150 ml of water for every kg of glucose [$\nu = 45$ Poise]
3. Glu_175 - 175 ml of water for every kg of glucose. [$\nu = 100$ Poise]

After the fluids were prepared, we added a few drops of blue ink to them for clear image analysis. The inclination of the ramp was adjusted to the required value. Data was collected for 3 different angles of inclination, i.e., $6°$, $16°$ and $25°$. We made use of a wooden ruler and trigonometry to measure the angle.

Before beginning the experiment, the glass surface of the ramp was thoroughly cleaned with surf water and wiped dry. Then, for a particular angle of inclination, 500 ml of a particular viscous fluid was carefully transferred from the storage container to the reservoir at the head of the ramp. The inclined ramp was carefully levelled before collecting any data. We attached a second reservoir at the back end of the apparatus, at the head of the ramp, behind the first reservoir. We added coloured water to this reservoir and by observing the meniscus of this coloured water, we could accurately level the inclined ramp.

The inclination of the camera was matched to the angle of inclination of the ramp to avoid warped images of the flow. Once the setup was ready, the video recording was turned on and the reservoir gate was unhooked. The three attached springs opened the entire length of the gate at once with a snap and the entire volume of fluid started flowing down the slope.

Great care was taken to ensure that the flow starts with a uniform horizontal flow front that spanned the entire width of the ramp. As the flow progressed, after a point, instability kicked in and led to the formation of wave-like instabilities that grew in amplitude with time. The surface of the ramp was cleaned with soap-water before repeating the experiment for the same fluid at other angles. In the case of glucose solutions, we found better results by just clearing the surface of excess fluid with a wiper, without the need for cleaning and drying with soap water. Similarly, data was collected for all the three fluids at each of the three angles.

Challenges and Solutions

1. Initially, the reservoir was placed such that the fluid was made to flow from its surface when the level of fluid in the reservoir became more than its height (this is essentially the second reservoir which we later used for levelling). We made a gravity pump for controlling the level of water in the reservoir and used another DC pump to feed the fluid into the gravity pump from our external containers. This led to immense hurdles in achieving an initial horizontal fluid-front. This happened due to numerous reasons:

(a) Since the level of fluid in the reservoir had to be raised by means of a gravity pump, fluid began to flow onto the ramp earlier from the region where the pipe attached to the pump was placed, unlike the regions further away from the pipe.

(b) The DC pump was not efficient and released the fluid in jerks, causing the entire surface of the fluid to remain unstable. Similarly, the height of the container that worked as a gravity pump had to be manually adjusted. This was not smooth and could not control the level of fluid in the reservoir efficiently.

(c) Moreover, the edge of the reservoir did not have the same level of smoothness at all points leading to variations in surface tension along its length. As a result, the flow was uneven and the experiment could not proceed.

In order to overcome this hurdle, we redesigned the setup and placed the reservoir such that the fluid would flow from the bulk of the reservoir when the gate in opened, instead of overflowing from the surface. We would wait for the pressure to equalize at every point in the reservoir before opening the gate. As a result, the fluid flow was uniform and a horizontal fluid-front was achieved.

2. Mixing water with glucose while preparing the glucose solutions led to the formation of a large number of air bubbles. The problem also arose while mixing blue ink with the prepared solutions or while transferring the solutions from one container to another. The presence of air bubbles in our specimen could have resulted in inaccurate and false data. Therefore, we waited for the required time to allow the air bubbles to escape before proceeding with the experiments.

3. We noticed that the different techniques applied to clean the sloping surface did affect the flow to some extent. While we cleaned the surface with soap-water every time before recording the flow of glycerine, we found that better results could be obtained without using soap-water for the glucose solutions. In the case of glucose solutions, we simply wiped away the excess fluid on the surface using a wiper. However, not many trials were conducted to verify this claim.

4. We often encountered leakages in the apparatus which were detrimental for our experiment. We used silicon gum in most cases to plug the leakages. Initially, the gate of the reservoir leaked fluid from its bottom edge and that could not be fixed using silicon gum as the gate had to remain detachable from below. In this case, we attached a thin rubber strip to the bottom of the gate to avoid leakages.

Analysis

The videos that were recorded for the flow of each fluid and at each angle of inclination were sorted and studied. From amongst the numerous videos captured, we chose those that provided us with the best results. Some videos had to be discarded due to issues related to levelling, focus, etc.

We then prepared a Python code using the OpenCV and Matplotlib libraries. We tracked the horizontal flow-front seen initially (stable-flow regime) during the flow and then the finger-like instabilities (unstable regime) after they had kicked in. The CSRT tracker in the OpenCV library was used for this purpose. The displacement of the fluid front at various points was carefully tracked at each time step and the data was then analyzed. We encountered some uncertainty in precisely determining *when* exactly can we characterize a boundary between the stable and instable regimes. We shall discuss an analytical technique we developed for this characterization in the sections ahead. The following are the four types of analysis we performed:

Stable flow with time

A de-dimensionalized graph motivated by relation 1 was plotted.

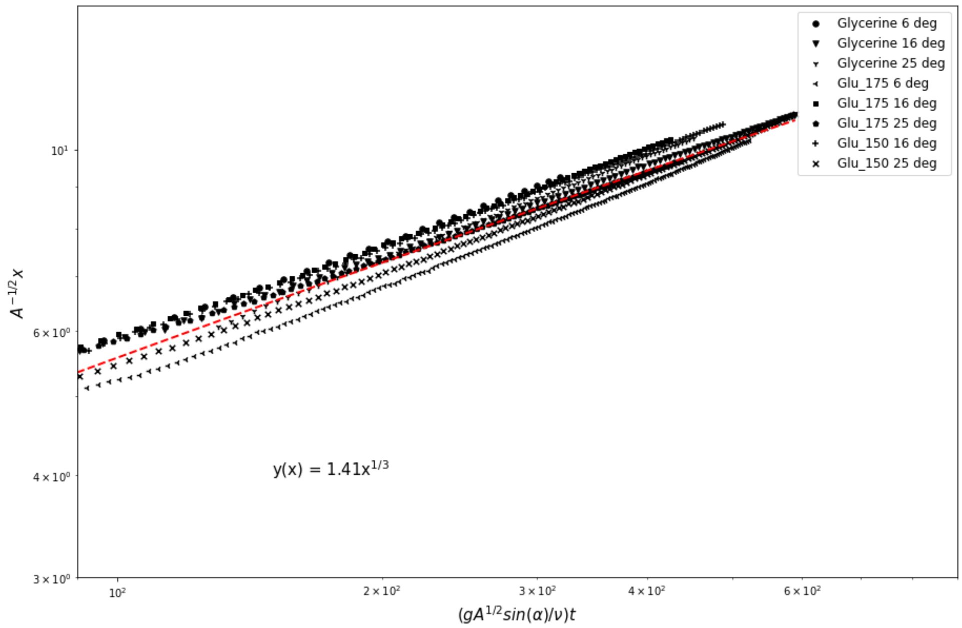

Figure 2: Non-dimensional length of stable flow as a function of non-dimensional time. Verification of results obtained by Huppert (1982).

Wavelength of projections

A de-dimensionalized graph motivated by relation 2 was plotted. Due to lack of surface tension measurements for the glucose liquids, we were only able to perform this analysis for glycerine.

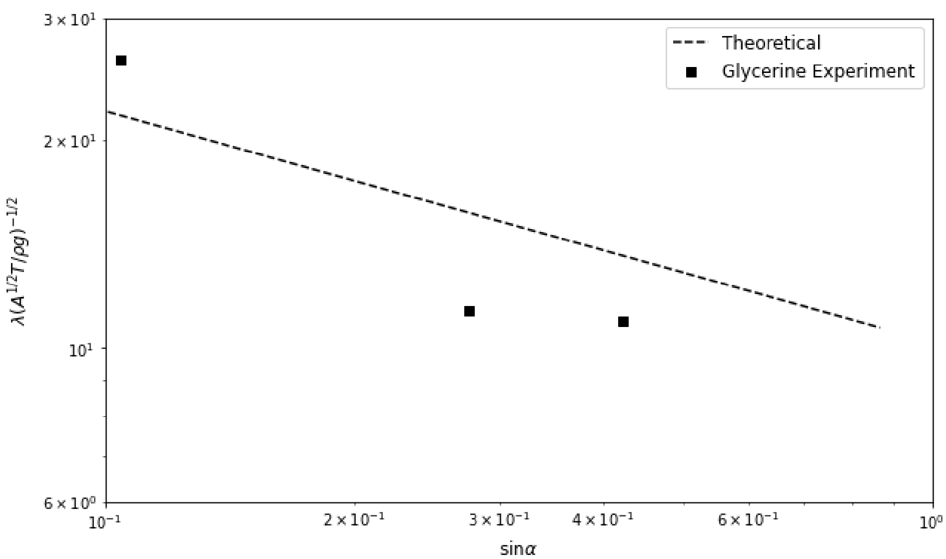

Figure 3: Non-dimensional wavelength of projections as a function of the sine of the angle of inclination.

Fastest-growing mode

It is common practice in non-equilibrium statistical mechanics to perform a fastest-growing mode analysis of the instabilities in a system to inspect which modes dominate in the late-time behaviour. Here, we observe instabilities in the fluid front. We use edge-detection algorithms from OpenCV in Python to detect the fluid front at increasing time steps. The edge-detected data has several irregularities which are smoothened using a Savitzky Golay filter algorithm. Next, the detected front is Fourier transformed to obtain the distribution of the various modes. Analysis at successive time-steps gives the fastest growing mode.

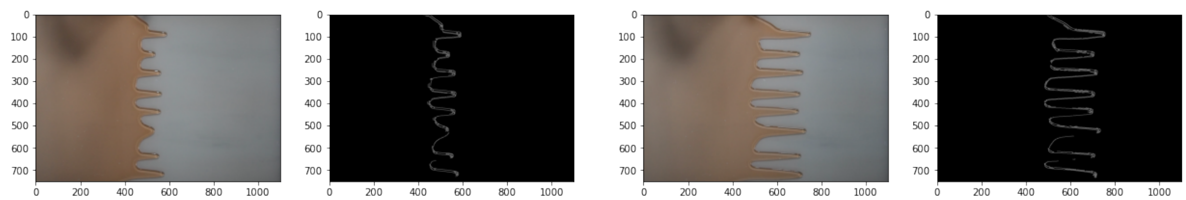

Figure 4: Edge Detection using OpenCV in Python

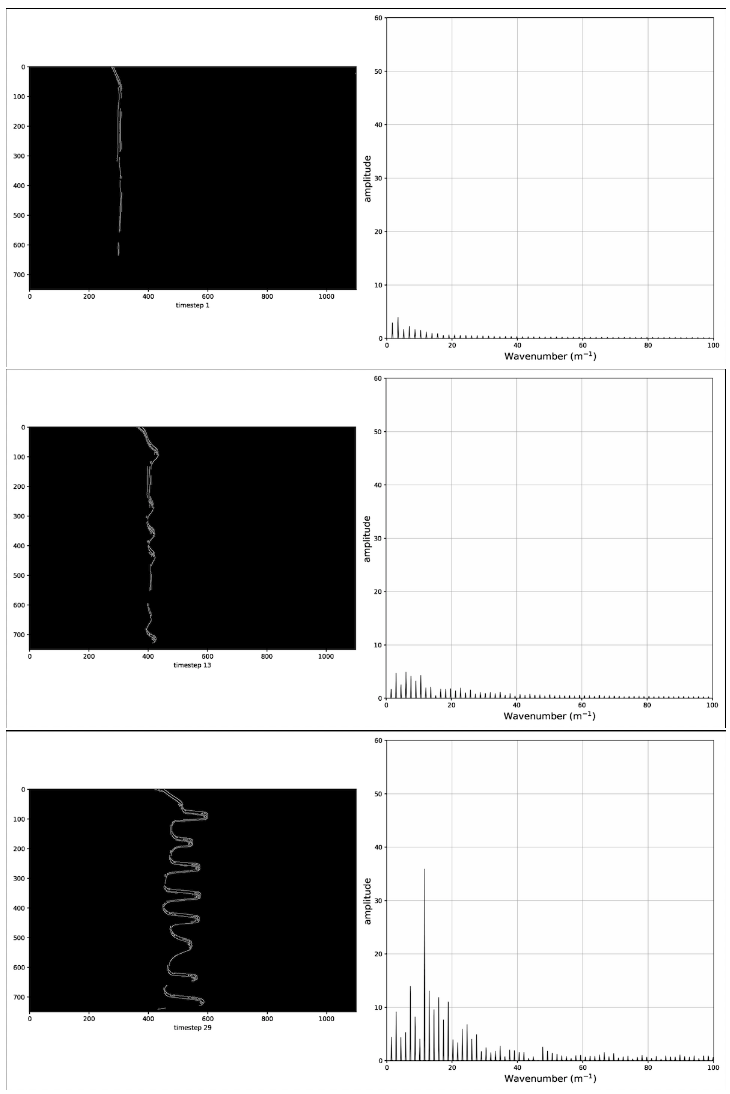

Figure 5: The fastest growing mode in the fluid front is found to be corresponding to wavelength 8.3 cm for Glu_175 flowing at an incline of 16°.

Phase transition perspective

Characterization of the stable flow and unstable flow regimes, and demarkation of their boundary was found to be an interesting problem. We use edge-detection to detect the fluid front, find the standard deviation of this front in the direction of the flow, and plot to obtain a graph which shows the increasing standard deviation of the fluid front with time. This is performed particularly during the transition from stable flow to unstable flow.

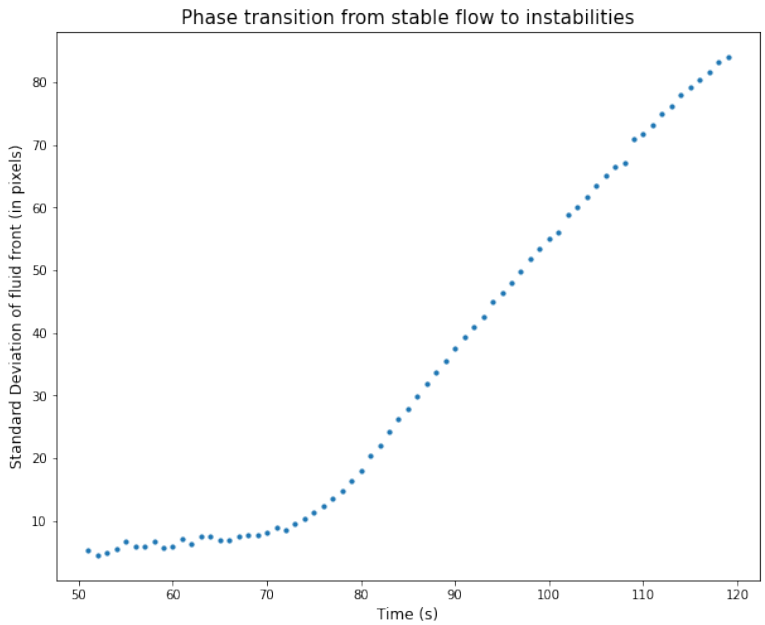

Figure 6: Standard deviation of the fluid front as a function of time for Glu_175 flowing at an incline of 16° exhibits a phase transition-like behaviour. The knee of the plot may be used to characterize a transition from stable flow to unstable flow.

It may be noted that a further illuminating analysis of similar nature may be to plot the standard deviation against the length travelled by the fluid front. This would shed light on Huppert's observation that the instabilities occur after the fluid has travelled a length proportional to $A^{1/2}$. We would thus observe graphs for fluids with different viscosities and at different angles of inclination collapse into one for a constant volume.

Results

The graph of dimensionless length travelled by the fluid front as a function of dimensionless time in the stable regime (see figure 2) verifies expression 1, and agrees with Huppert's observations (1982). This confirms the hypothesis that the balance between the viscous and gravitational forces determine the dynamics in this regime. The graph for wavelengths of projections (see figure 3) does not seem to agree very well with the theoretical predictions. This may be due to insufficient data or large experimental error. However, it should be noted that a study by Silvi *et al.* (1984) also found deviation from Huppert's theoretical prediction (expression 2).

The fastest growing mode analysis using Fourier transforms of the fluid front for Glu_175 flowing on a 16° incline successfully gives the dominant mode as observed, as well as sheds light on the growth of other modes. Such analysis may find use when formulating the emergence of instabilities using statistical mechanics. The time evolution of the standard deviation of the fluid front provides a method to *precisely* determine the transition from stable flow regime to unstable flow. This method can be used in further studies to rigorously define the two regimes.

Further, we illustrate the position (fluid front) versus time plots for all the experiments we performed in Appendix A. We illustrate both, the stable regime and the unstable regime by plotting the position of the fluid front for the former, and the position of the various individual projections for the latter. Comparison of the plots for various cases provides the following observations:

1. Different projections in a single experiment tend to have different flow-rates. This seems to depend on their respective sizes (thickness) from experimental observations.
2. Towards the end of each experiment, the various projections have a spread in their positions. However, this spread is of the same length scale for all the experiments, regardless of the fluid viscosity and the angle of inclination.
3. While the instabilities kick in after different elapsed times for different experiments, they always occur after the same length is travelled by the fluid front. This is in agreement with Huppert's observation that the maximum length travelled in the stable regime is proportional to $A^{1/2}$. Since all our experiments were conducted with the same volume of liquid, 500 mL, we expect this length scale to remain constant.

Plan Ahead

The exciting results acquired here opens up avenues for many associated studies and experiments in coming times. To summarize the conditions of this particular experiment, we used Newtonian fluids of varying viscosities and data was acquired for constant-volume flow. In the coming days, we plan to carry out the same experiment under the following new conditions:

1. Non-Newtonian fluids at constant-volume flow
2. Non-Newtonian fluids at constant-flux flow
3. Newtonian fluids at constant-flux flow

Further, we intend to explore the process of emergence of instabilities and characterize them using the new analytical techniques developed here. A detailed comparative study of all the cases will hopefully provide us with new insights.

Acknowledgement

Firstly, we would like to thank Professor Pramoda Kumar for accepting our proposal for this Independent Study Module and guiding us through the process. His guidance and insights helped us tremendously in coming up with the desired results. Secondly, we thank and appreciate Pradeep Bhaiya for his brilliant work in helping us prepare the framework of the experimental setup and being forever present with his experience and ingenious ideas. We could overcome most of the logistical and engineering challenges only because of his sheer dedication and years of experience. In short, this experiment would not have been possible without Pradeep Bhaiya's presence. Lastly, we would like to thank Sudarshana Banerjee for making the procurement of items effortless, despite the extremely difficult times we find ourselves in, and thereby helping us complete our work on time.

References

1. Huppert, Herbert E. *"Flow and instability of a viscous current down a slope."* Nature 300.5891 (1982): 427-429.
2. Silvi, N., and E. B. Dussan V. *"The rewetting of an inclined solid surface by a liquid."* The Physics of fluids 28.1 (1985): 5-7.

Appendix A

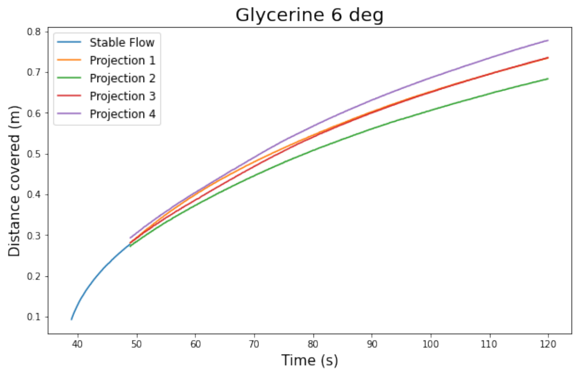

Glycerine 6 deg
Stable Flow
Projection 1
Projection 2
Projection 3
Projection 4
Distance covered (m)
Time (s)

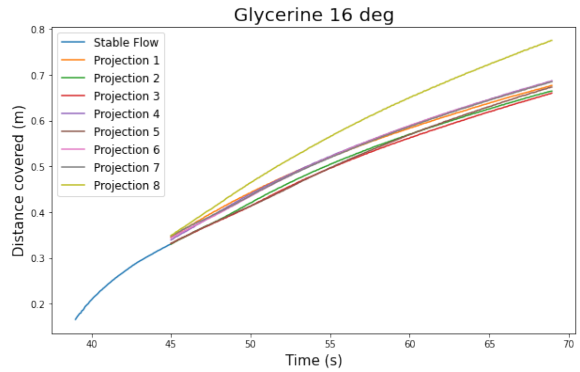

Glycerine 16 deg
Stable Flow
Projection 1
Projection 2
Projection 3
Projection 4
Projection 5
Projection 6
Projection 7
Projection 8
Distance covered (m)
Time (s)

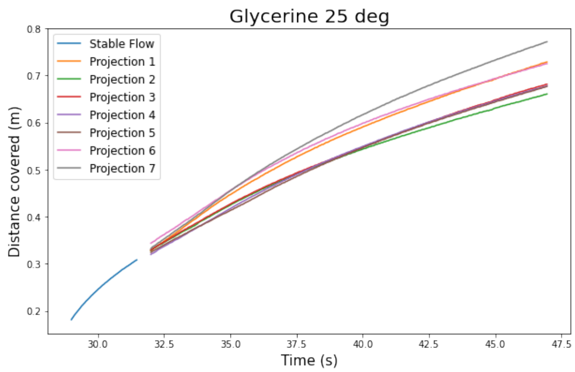

Glycerine 25 deg
Stable Flow
Projection 1
Projection 2
Projection 3
Projection 4
Projection 5
Projection 6
Projection 7
Distance covered (m)
Time (s)

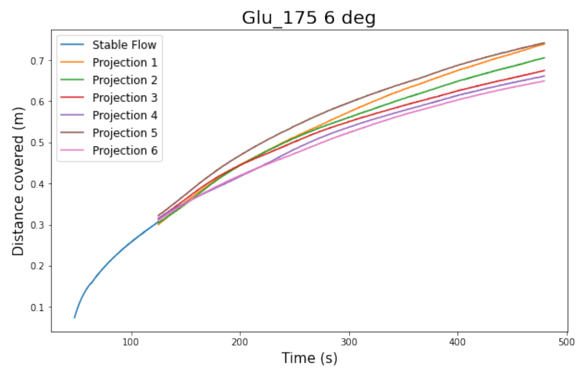

Glu_175 6 deg
Stable Flow
Projection 1
Projection 2
Projection 3
Projection 4
Projection 5
Projection 6
Distance covered (m)
Time (s)

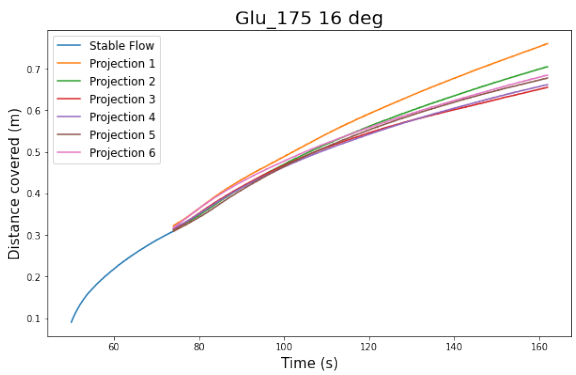

Glu_175 16 deg
Stable Flow
Projection 1
Projection 2
Projection 3
Projection 4
Projection 5
Projection 6
Distance covered (m)
Time (s)

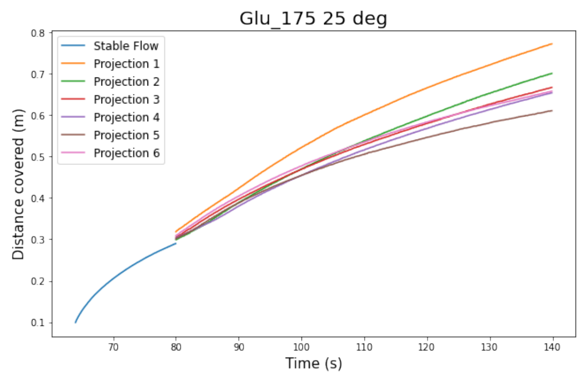

Glu_175 25 deg
Stable Flow
Projection 1
Projection 2
Projection 3
Projection 4
Projection 5
Projection 6
Distance covered (m)
Time (s)

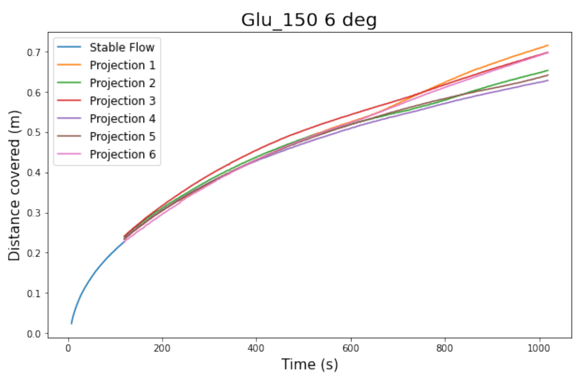

Glu_150 6 deg
Stable Flow
Projection 1
Projection 2
Projection 3
Projection 4
Projection 5
Projection 6
Distance covered (m)
Time (s)

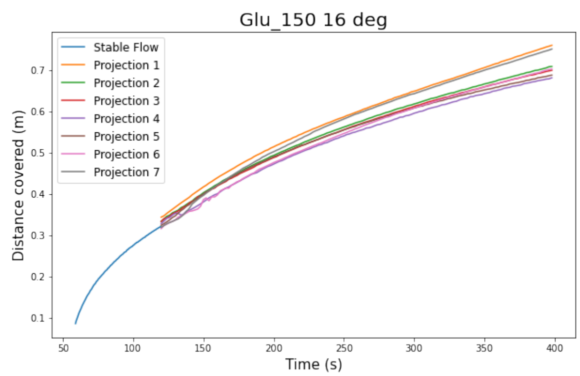

Glu_150 16 deg
Stable Flow
Projection 1
Projection 2
Projection 3
Projection 4
Projection 5
Projection 6
Projection 7
Distance covered (m)
Time (s)

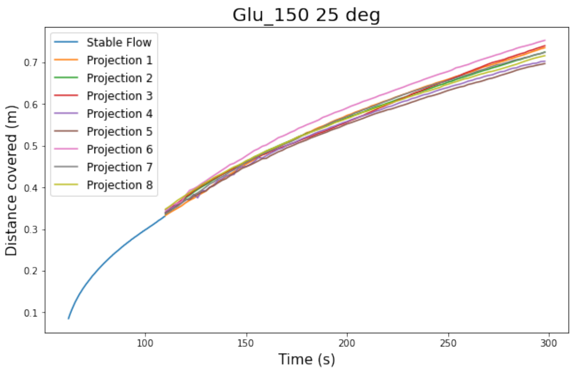
Glu_150 25 deg
Stable Flow
Projection 1
Projection 2
Projection 3
Projection 4
Projection 5
Projection 6
Projection 7
Projection 8
Distance covered (m)
Time (s)

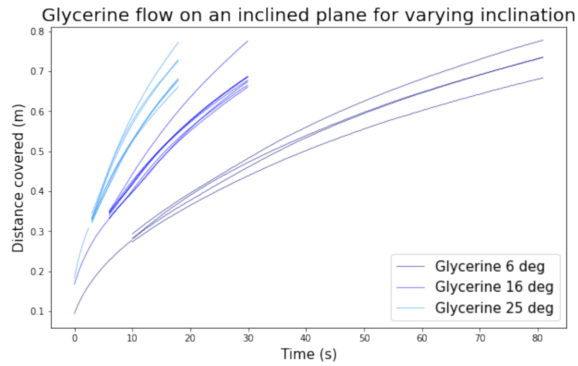
Glycerine flow on an inclined plane for varying inclination
Glycerine 6 deg
Glycerine 16 deg
Glycerine 25 deg
Distance covered (m)
Time (s)

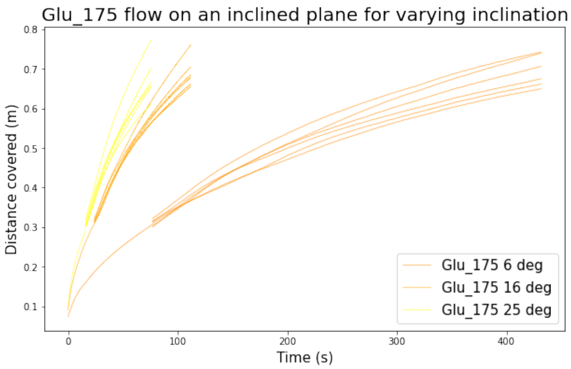
Glu_175 flow on an inclined plane for varying inclination
Glu_175 6 deg
Glu_175 16 deg
Glu_175 25 deg
Distance covered (m)
Time (s)

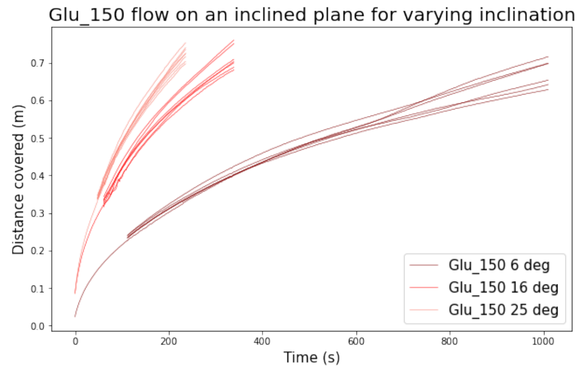
Glu_150 flow on an inclined plane for varying inclination
Glu_150 6 deg
Glu_150 16 deg
Glu_150 25 deg
Distance covered (m)
Time (s)

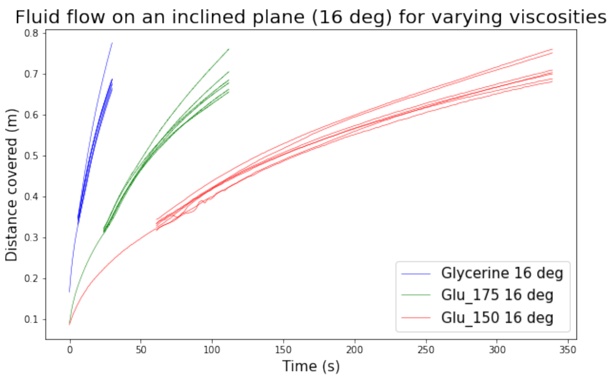
Fluid flow on an inclined plane (16 deg) for varying viscosities
Glycerine 16 deg
Glu_175 16 deg
Glu_150 16 deg
Distance covered (m)
Time (s)

Appendix B

This appendix contains images of the experimental setup.

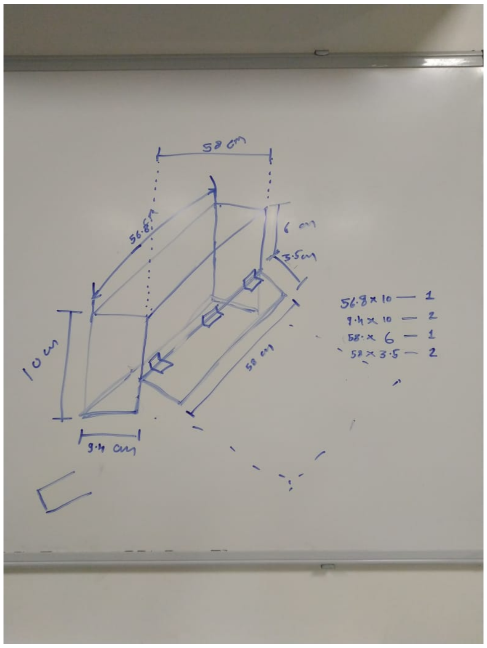

Figure 7: Prototype of the reservoir design

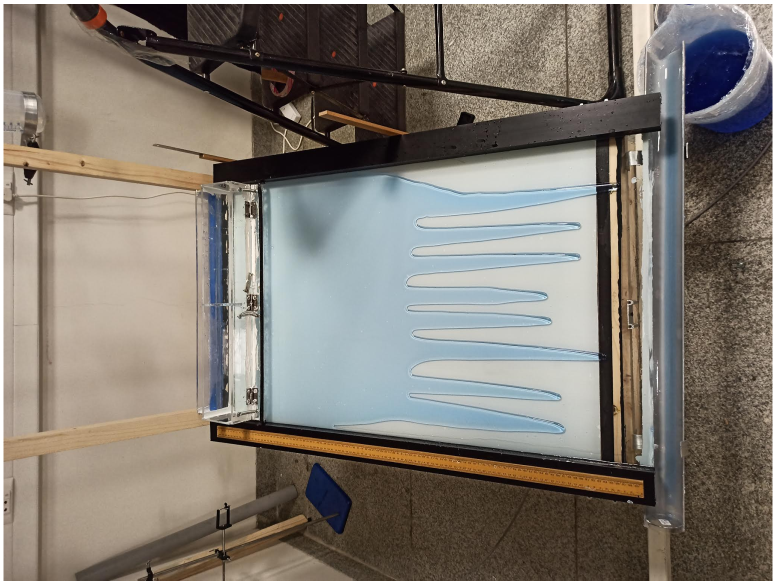

Figure 8: Snapshot of the experiment

(a) Wooden framework

(b) Framework with Ramp

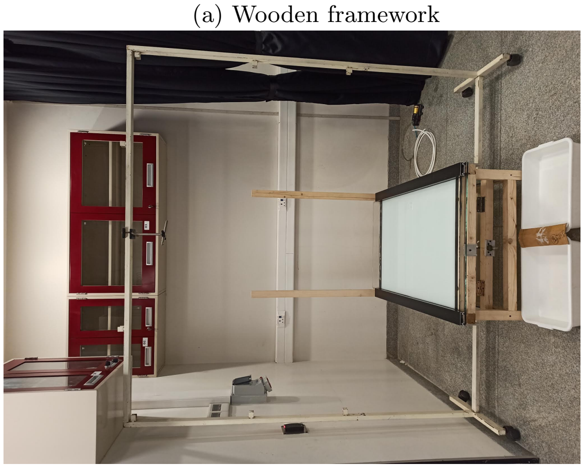

(c) Setup with camera stand

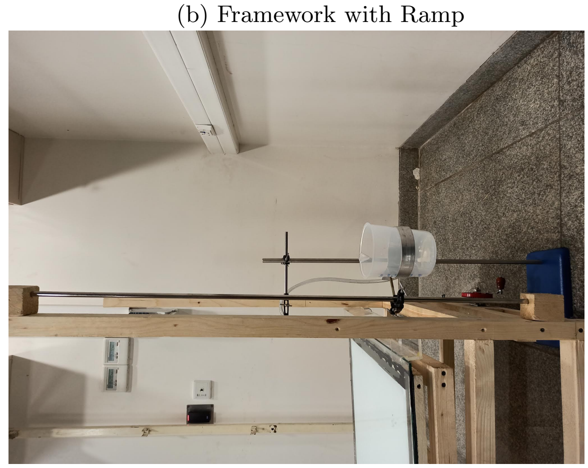

(d) Gravity pump

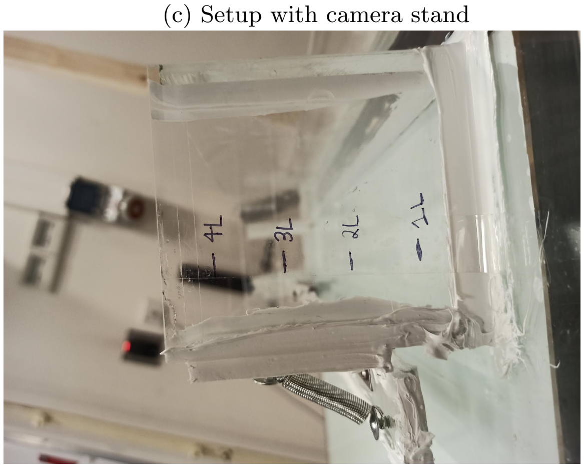

(e) Reservoir

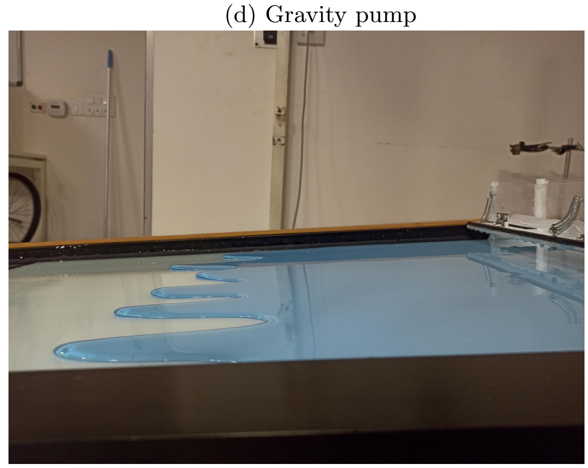

(f) Lateral view of fluid flow (unstable regime)